International Journal of General Medicine

Dovepress
Taylor & Francis Group

Open Access Full Text Article

ORIGINAL RESEARCH

Alterations of White Matter Microstructure in Primary Aldosteronism Patients With Normal Cognitive Functioning Using Diffusion Tensor Imaging

Weijie Chen[1,2,*], Simin Deng[3,*], Heng Li[2], Yu Zhao[2], Yuntao Tian[2], Yiqiang Yuan[1,4]

[1]The Second School of Clinical Medicine, Southern Medical University, Guangzhou, People's Republic of China; [2]Department of Cardiology, Dongguan Tung Wah Hospital, Guangdong, People's Republic of China; [3]Department of Rehabilitation Medicine, Dongguan Eighth People's Hospital, Guangdong, People's Republic of China; [4]Department of Cardiology, The Seventh People's Hospital of Zhengzhou, Henan, People's Republic of China

*These authors contributed equally to this work

Correspondence: Yiqiang Yuan, The Second School of Clinical Medicine, Southern Medical University, Guangzhou, 510515, People's Republic of China, Tel +86-0371-61205666, Fax +86 0371 86615553, Email zzqyyuanyiqiang@126.com

Objective: To detect white matter microstructural alterations in patients with primary aldosteronism (PA) with normal cognitive function using diffusion tensor imaging (DTI).

Methods: This study included PA patients and normotensive healthy controls (HCs). MRI (T1-weighted) and DTI data were collected for all participants. Using the Johns Hopkins University white matter fiber tractography template, we calculated the values of fractional anisotropy (FA), axial diffusivity (AD), radial diffusivity (RD), and mean diffusivity (MD).

Results: Compared to the HC group, the PA group showed significant increases in AD in cingulum bundle cingulate part (CgC.R), forceps minor (FMi), bilateral inferior fronto-occipital fasciculi (IFO), and right temporo-superior longitudinal fasciculus (tSLF.R); RD in left IFO (IFO.L) and right superior longitudinal fasciculus (SLF.R); and MD in FMi, IFO.L, right IFO (IFO.R) and SLF.R.

Conclusion: Compensatory white matter alterations occur in PA patients before cognitive impairment. These alterations may serve as early imaging biomarkers for PA-related brain function impairment, highlighting the importance of advanced neuroimaging for early diagnosis and intervention.

Keywords: white matter microstructural alterations, diffusion tensor imaging, primary aldosteronism, cognitive

Introduction

Primary aldosteronism (PA) is a prevalent form of secondary hypertension, affecting approximately 5% to 10% of hypertensive patients.[1,2] The clinical manifestations of PA arise from excessive aldosterone secretion by the adrenal cortex, leading to increased sodium and water retention and accelerated potassium excretion, which in turn elevates blood pressure.[3] If left untreated, PA significantly elevates the risk of coronary heart disease, left ventricular hypertrophy, heart failure, and stroke.[4] While numerous studies have documented the heightened risk of cardiovascular complications in PA patients, there is a paucity of research examining the impact of PA on brain structure and function, particularly regarding the integrity of white matter.[5]

White matter, composed of tightly connected nerve fibers, plays a critical role in transmitting signals between brain regions, which is essential for maintaining normal cognitive functions. Damage or degenerative changes in white matter are directly associated with various neurological diseases and cognitive decline.[6] Diffusion tensor imaging (DTI) technology allows us to observe the orientation and integrity of white matter fibers, offering valuable insights into brain structural connectivity and neural fiber architecture.[7] DTI assesses the diffusion behavior of water molecules in

Received: 1 November 2024
Accepted: 19 February 2025
Published: 25 February 2025

white matter through four main metrics: fractional anisotropy (FA), axial diffusivity (AD), radial diffusivity (RD) and mean diffusivity (MD), which are vital for evaluating the microstructural state of white matter.[8] FA indicates the coherence of fiber bundle direction, reflecting the tendency of water molecules to diffuse along specific directions;[9] MD represents the average rate of water molecule diffusion in all directions, indicating the overall diffusion capacity of water molecules in brain tissue;[10] AD relates to the diffusion rate along the fiber axis, reflecting axonal integrity;[9] and RD measures diffusion perpendicular to the fiber axis, primarily associated with myelin sheath condition.[9]

Previous DTI studies on hypertensive patients have primarily focused on high-signal areas in white matter. These studies revealed a link between high-signal density in white matter and cognitive impairment,[11] and found that this high signal intensity correlates with systolic blood pressure (SBP)[12] and pulse pressure.[13] Additionally, these studies highlighted the influence of age and gender on white matter microstructure. For example, in women, higher SBP and pulse pressure were negatively correlated with high-signal intensity in the left corticospinal tract (CST), superior longitudinal fasciculus (SLF), temporo-superior longitudinal fasciculus (tSLF), and right parahippocampal gyrus. In contrast, in men, higher diastolic blood pressure (DBP) was positively correlated with high-signal intensity in the bilateral CST, left inferior longitudinal fasciculus, and inferior fronto-occipital fasciculus (IFO).[14] However, these findings were predominantly focused on hypertensive patients and did not explore patients with the different subtypes of hypertension. These findings, however, have predominantly focused on essential hypertension (EHT), with limited investigation into the effects across hypertension subtypes. As a form of secondary hypertension, PA may affect brain functions by impairing blood-brain barrier integrity and inducing neuroinflammation,[15] with a higher risk of cardiovascular and cerebrovascular complications than EHT,[16] raising the question of whether PA patients are more vulnerable to white matter damage. Early detection of such changes is clinically significant, as it may help identify early markers of cognitive decline and guide timely interventions. To explore this, we extended previous research[17] on EHT to specifically assess PA patients who had not experienced cerebrovascular events and demonstrated normal cognitive function. By employing DTI to evaluate white matter microstructural parameters, we aimed to uncover unique patterns of microstructural white matter damage in PA, providing fresh insights into the mechanisms of white matter injury in this population.

This study, assuming that PA patients may exhibit white matter microstructural alterations with normal cognitive function, included both PA patients and normotensive healthy controls (HC). We collected magnetic resonance imaging (MRI) (T1-weighted images) and DTI data from the participants. Utilizing the Johns Hopkins University (JHU) white matter fiber tractography template and template segmentation techniques, this study aimed to elucidate the underlying mechanisms of PA's impact on brain cognitive function. By comparing the differences in fiber bundle DTI parameters based on regions of interest (ROI) between the two groups, we sought to provide new research perspectives. This methodological framework aimed to determine whether PA patients experience white matter microstructural alterations before cognitive impairment becomes evident and to identify the exact manifestations of such alterations, thereby providing theoretical support for future prevention and treatment measures.

Materials and Methods

Study Subjects

This study was conducted in the Department of Cardiovascular Medicine at Dongguan Tung Wah Hospital. Approval was obtained from the Institutional Ethics Committee (Ethics Approval Number: 2021-KY-034), and the study was registered with the Chinese Clinical Trial Registry (Registration Number: ChiCTR2100053166). The study was conducted in compliance with the principles outlined in the Declaration of Helsinki. Informed consent was obtained from all participants.

From November 2021 to November 2022, 418 hypertensive patients were screened, of whom 42 were diagnosed with PA and 42 were recruited as HC. Based on the exclusion criteria, 12 PA patients were excluded: 6 had type 2 diabetes mellitus, 4 had coronary heart disease, and 2 had atrial fibrillation. The remaining 30 PA patients underwent cranial MRI scans, resulting in the exclusion of 8 additional patients due to abnormal cranial MRI findings (3 with stroke and 5 with cerebral white matter ischemic lesions). Nine HC subjects were excluded due to abnormal cranial MRI findings (2 with

stroke and 7 with cerebral white matter ischemic lesions). Consequently, 22 PA patients and 33 hC subjects with normal cranial MRI scans were included in the study.

Participants were included based on the following criteria:

1. HC Group: SBP <140 mmHg and DBP <90 mmHg and without a history of hypertension diagnosis or treatment with antihypertensive drugs. PA Group: Patients diagnosed with PA. All enrolled PA patients were diagnosed through a comprehensive diagnostic process.[18] Initially, patients were screened using the aldosterone-to-renin ratio (ARR), with a standing ARR greater than 38 considered indicative of PA. For those with positive screening results, the saline infusion test (SIT) was conducted as the confirmatory test. Patients were diagnosed with PA if their post-infusion plasma aldosterone concentration (PAC) remained above 100 pg/mL. This process ensured that all PA patients had elevated ARR and reduced plasma renin concentration, with the diagnosis confirmed through SIT, with detailed procedures described in Appendix A.

2. Mini-mental state examination (MMSE) scores ranging from 24 to 30 were recorded. The study team used an unauthorized version of the Chinese MMSE without permission, but this issue has been rectified with psychological assessment resources (PAR).

3. Clinical dementia rating (CDR) score of 0.

Exclusion criteria were as follows:

1. Cognitive abnormalities such as dementia, diagnosed neurological or psychiatric disorders, and use of drugs affecting cognitive function.

2. Abnormal cranial MRI findings, including stroke, seizure, and Parkinson's disease.

3. Other types of secondary hypertension.

4. Other significant health issues such as tumors, heart failure, renal insufficiency, liver dysfunction, hematological diseases, chronic pulmonary infections, diabetes mellitus, atrial fibrillation or flutter, and other severe internal medicine diseases.

5. Structural MRI employed a 3D magnetization-prepared rapid gradient-echo T1-weighted sequence to exclude white matter lesions, cerebral hemorrhage, ischemic foci, or other abnormalities.

6. Scans with head movement greater than or equal to 2° or 2 mm were excluded.

MRI Data Acquisition

Structural MRI and DTI data were collected for both the HC and PA groups using a 3.0-T MRI scanner (Siemens Skyra, Germany) at Dongguan Tung Wah Hospital. DTI used a single-shot echo-planar imaging sequence. Participants were scanned in the supine position with foam pads to minimize head movement. The DTI scanning parameters were as follows: repetition time (TR) = 3700 ms, echo time (TE) = 92 ms, 25 slices, spatial resolution = 1.7×1.7 × 4.0 mm^3, 12 zero-weighted images (b = 0 s/mm^2), 60 nonlinear diffusion-weighted directions (b = 1000 s/mm^2), acquisition matrix = 128 × 128, and field of view (FOV) = 220×220 mm^2.

DTI Data Processing

DTI data preprocessing was performed using PANDA (Pipeline for Analyzing Brain Diffusion Images, http://www.nitrc.org/projects/panda/) software.[19] The main steps included:

1.Converting raw DICOM data to NIFTI format.

2.Removing non-brain tissue.

3.Correcting for eddy current distortions and head movements using b = 0 s/mm^2 images.

4.Calculating the diffusion tensor characteristics for each voxel and estimating FA, MD, AD, and RD for both groups.

Specific ROI based analyses were conducted using a current white matter map to identify differences in DTI parameters between the HC and PA groups. Nonlinear registration techniques aligned FA images to the FMRIB-58 FA template in Montreal Neurological Institute (MNI) space, generating the corresponding spatial transformation matrix. This matrix was then applied to the spatial registration of MD, AD, and RD. Further, spatially normalized MD, AD, and RD images were smoothed using a 6 mm full-width at half maximum (FWHM) Gaussian kernel to balance noise reduction and spatial resolution, ensuring accurate evaluation of white matter microstructural parameters. The white

matter template used in this study was the JHU ICBM DTI-81 atlas (http://cmrm.med.jhmi.edu/),[20] which includes 20 white matter fiber tract regions. This atlas was selected for its anatomical accuracy, comprehensive coverage of major white matter tracts, and widespread use in DTI studies, ensuring comparability and reproducibility with prior research. For each ROI in the atlas, the mean FA, MD, AD and RD values were calculated.

Statistical Analysis

Statistical analysis was conducted using SPSS 26.0 software to compare demographic and clinical data between the PA and HC groups. For continuous variables, independent samples t-tests were used; for categorical variables, the χ^2-test was applied. A p-value <0.05 was considered statistically significant. DTI parameter comparisons between the PA and HC groups were performed using independent samples t-tests in SPSS software. Bonferroni corrections were applied to account for multiple comparisons. Post-hoc multiple comparisons were conducted with sex, age, and education level as covariates, setting the significance threshold at $p < 0.05$.

Results

Demographic and Clinical Characteristics

Table 1 summarizes the demographic, clinical, and neuropsychological characteristics of the study subjects in both groups. The PA group exhibited significantly higher SBP (137.36±11.05 VS 114.12±6.99 mmHg), DBP (137.36±11.05 VS 114.12±6.99 mmHg), interventricular septum thickness at end-diastole (IVSd) (10.50±1.10 VS 9.58±0.90 mm), and left ventricular posterior wall thickness at end-diastole (LVPWd) (10.09±1.06 VS 9.39±0.86 mm) compared to the HC group. Additionally, the PA group (3.58±0.36 VS 4.09±0.26 mmol/L) had significantly lower blood potassium levels than the HC group ($p < 0.05$).

Table 1 Demographic Differences Between the PA and HC Groups ($\bar{x} \pm s$)

Demographic Information	PA (n=22)	HC (n=33)	*p* value
Age (years)	49.77 ± 9.48	48.18 ± 8.60	0.522
Gender (M/F)	8/14	19/14	0.128
Years of Education	10.36 ± 3.26	10.97 ± 3.05	0.485
BMI (kg/m^2)	24.29 ± 2.65	24.31 ± 3.20	0.981
Smoking History	3	10	0.137
SBP (mmHg)	137.36 ± 11.05	114.12 ± 6.99	**0.000***
DBP (mmHg)	84.50 ± 9.78	69.42 ± 5.12	**0.000***
Creatinine (umol/L)	65.96 ± 17.65	72.95 ± 16.08	0.135
LDL-C (mmol/L)	2.84 ± 0.77	3.05 ± 0.76	0.685
TG (mmol/L)	1.68 ± 1.14	1.81 ± 1.01	0.666
Blood Potassium (mmol/L)	3.58 ± 0.36	4.09 ± 0.26	**0.000***
Standing ARR	107.36 ± 148.25	–	–
PAC before SIT (pg/mL)	251.31± 194.15	–	–
PAC after SIT (pg/mL)	173.99 ± 103.94	–	–
LAD (mm)	31.32 ± 4.21	30.18 ± 2.71	0.228
LVDd (mm)	45.90 ± 3.53	45.52 ± 2.74	0.644

(*Continued*)

Table 1 (Continued).

Demographic Information	PA (n=22)	HC (n=33)	*p* value
IVSd (mm)	10.50 ± 1.10	9.58 ± 0.90	**0.001***
LVPWd (mm)	10.09 ± 1.06	9.39 ± 0.86	**0.010***
LVEF (%)	65.77 ± 3.96	66.73 ± 4.13	0.398
MMSE	28.18 ± 1.71	28.96 ± 1.42	0.081

Note: The data is presented as mean ± standard deviation. Bold and * indicates a significant difference between groups (p value < 0.05).

Abbreviations: PA, primary aldosteronism; HC, healthy controls; M, male; F, female; BMI, body mass index; SBP, systolic blood pressure; DBP, diastolic blood pressure; LDL-C, low-density lipoprotein cholesterol; TG, triglycerides; ARR, aldosterone-to-renin ratio; PAC, plasma aldosterone concentration; SIT, saline infusion test; LAD, left atrial diameter; LVDd, left ventricular end-diastolic diameter; IVSd, interventricular septum thickness at end-diastole; LVPWd, left ventricular posterior wall thickness at end-diastole; LVEF, left ventricular ejection fraction; MMSE, Mini-mental state examination.

DTI Parameters Based on ROIs

Comparison of FA Values

The comparison of FA values between the PA and HC groups did not reveal any significant differences, as detailed in Table 2.

Table 2 Comparison of FA Values Between the Two Groups Based on ROIs ($\bar{x}$ ± s)

ROIs	PA	HC	*p* value	t value
ATR.L	0.298 ± 0.014	0.303 ± 0.017	0.8347	−0.2097
ATR.R	0.302 ± 0.014	0.305 ± 0.014	0.8822	0.1489
CST.L	0.466 ± 0.018	0.474 ± 0.014	0.3019	−1.0426
CST.R	0.456 ± 0.019	0.461 ± 0.015	0.7127	−0.3702
CgC.L	0.361 ± 0.025	0.363 ± 0.027	0.3454	0.9521
CgC.R	0.315 ± 0.029	0.316 ± 0.005	0.3344	0.9741
CgH.L	0.232 ± 0.018	0.241 ± 0.028	0.2225	−1.2343
CgH.R	0.243 ± 0.024	0.247 ± 0.029	0.8494	−0.1909
FMa	0.466 ± 0.018	0.467 ± 0.023	0.2327	−1.2071
FMi	0.351 ± 0.015	0.357 ± 0.017	0.4832	−0.7061
IFO.L	0.339 ± 0.015	0.345 ± 0.016	0.3407	−0.9614
IFO.R	0.345 ± 0.016	0.349 ± 0.015	0.6137	−0.5078
ILF.L	0.336 ± 0.013	0.342 ± 0.016	0.1510	−1.4571
ILF.R	0.356 ± 0.017	0.359 ± 0.021	0.7851	−0.2740
SLF.L	0.290 ± 0.012	0.293 ± 0.014	0.8154	−0.2347
SLF.R	0.312 ± 0.015	0.319 ± 0.016	0.3255	−0.9924

(*Continued*)

https://doi.org/10.2147/IJGM.S499346

Table 2 (Continued).

ROIs	PA	HC	*p* value	t value
Unc.L	0.310 ± 0.018	0.307 ± 0.018	0.2402	1.1877
Unc.R	0.309 ± 0.022	0.314 ± 0.022	0.8758	−0.1570
tSLF.L	0.386 ± 0.031	0.379 ± 0.034	0.2583	1.1428
tSLF.R	0.473 ± 0.027	0.464 ± 0.040	0.2720	1.1100

Note: The data is presented as mean ± standard deviation.
Abbreviations: FA, fractional anisotropy; ROIs, regions of interest; PA, primary aldosteronism; HC, healthy controls; L, left; R, right; ATR, anterior thalamic radiation; CST, corticospinal tract; CgC, cingulum bundle cingulate part; CgH, cingulum bundle hippocampal part; FMa, forceps major; FMi, forceps minor; IFO, inferior fronto-occipital fasciculus; ILF, inferior longitudinal fasciculus; SLF, superior longitudinal fasciculus; Unc, uncinate fasciculus; tSLF, temporo-superior longitudinal fasciculus.

Comparison of AD Values

The comparison of AD values between the PA and HC groups showed significant differences. The PA group exhibited a significant increase in AD in the right cingulum bundle cingulate part (CgC.R) (0.0011±0.0000 VS 0.0010±0.0000), forceps minor (FMi) (0.0012±0.0000 VS 0.00118±0.0000), left IFO (IFO.L) (0.00113±0.0000 VS 0.00111±0.0000), right IFO (IFO.R) (0.00114±0.0000 VS 0.0012±0.0000), and tSLF.R (0.00122±0.0000 VS 0.00119±0.0000) compared to the HC group, as shown in Table 3 and Figures 1–3.

Table 3 Comparison of AD Values Between the Two Groups Based on ROIs ($\bar{x}$ ± s)

ROIs	PA	HC	*p* value	t value
ATR.L	0.0011 ± 0.0001	0.0011 ± 0.0001	0.7043	0.3815
ATR.R	0.0011 ± 0.0001	0.0011 ± 0.0001	0.2662	1.1236
CST.L	0.0012 ± 0.0000	0.0012 ± 0.0000	0.9285	0.0901
CST.R	0.0012 ± 0.0000	0.0012 ± 0.0000	0.3258	0.9917
CgC.L	0.0011 ± 0.0000	0.0011 ± 0.0000	0.7448	0.3272
CgC.R	0.0011 ± 0.0000	0.0010 ± 0.0000	**0.0316***	2.2077
CgH.L	0.0011 ± 0.0000	0.0011 ± 0.0000	0.5607	0.5855
CgH.R	0.0012 ± 0.0001	0.0012 ± 0.0001	0.3004	1.0457
FMa	0.0014 ± 0.0001	0.0014 ± 0.0001	0.4660	0.7344
FMi	0.0012 ± 0.0000	0.00118 ± 0.0000	**0.0430***	2.0735
IFO.L	0.00113 ± 0.0000	0.00111 ± 0.0000	**0.0103***	2.6615
IFO.R	0.00114 ± 0.0000	0.00112 ± 0.0000	**0.0164***	2.4781
ILF.L	0.0011 ± 0.0000	0.0011 ± 0.0000	0.8054	0.2476
ILF.R	0.0011 ± 0.0000	0.0011 ± 0.0000	0.0896	1.7292
SLF.L	0.0010 ± 0.0000	0.0010 ± 0.0000	0.1398	1.4991

(*Continued*)

Table 3 (Continued).

ROIs	PA	HC	*p* value	t value
SLF.R	0.0010 ± 0.0000	0.0010 ± 0.0000	0.0583	1.9355
Unc.L	0.0011 ± 0.0000	0.0011 ± 0.0000	0.1350	1.5179
Unc.R	0.0011 ± 0.0000	0.0011 ± 0.0000	0.1195	1.5823
tSLF.L	0.0011 ± 0.0000	0.0011 ± 0.0001	0.3451	0.9527
tSLF.R	0.00119 ± 0.0000	0.00122 ± 0.0000	**0.0488***	2.0172

Note: The data is presented as mean ± standard deviation. Bold and * indicates a significant difference between groups (p value < 0.05).

Abbreviations: AD, axial diffusivity; ROIs, regions of interest; PA, primary aldosteronism; HC, healthy controls; L, left; R, right; ATR, anterior thalamic radiation; CST, corticospinal tract; CgC, cingulum bundle cingulate part; CgH, cingulum bundle hippocampal part; FMa, forceps major; FMi, forceps minor; IFO, inferior fronto-occipital fasciculus; ILF, inferior longitudinal fasciculus; SLF, superior longitudinal fasciculus; Unc, uncinate fasciculus; tSLF, temporo-superior longitudinal fasciculus.

Comparison of RD Values

The comparison of RD values between the PA and HC groups revealed significant differences. The PA group demonstrated a significant increase in RD in the IFO.L (0.0007±0.0000 VS 0.0006±0.0000) and right SLF (SLF.R) (0.00064 ±0.0000 VS 0.00062±0.0000) compared to the HC group, as illustrated in Table 4, Figures 3 and 4.

Comparison of MD Values

The comparison of MD values between the PA and HC groups also showed significant differences. The PA group exhibited a significant increase in MD in the FMi (0.0009±0.0000 VS 0.0008±0.0000), IFO.L (0.00082±0.0000 VS 0.00080±0.0000), IFO.R (0.00081±0.0000 VS 0.00080±0.0000), and SLF.R (0.00077±0.0000 VS 0.00075±0.0000) compared to the HC group, as detailed in Table 5, Figures 3 and 5.

Discussion

This study utilized DTI technology to investigate the extent of white matter microstructural alterations in patients with PA. The results indicated significant changes in white matter integrity, evidenced by increased AD values in the CgC.R, FMi, bilateral IFO, and tSLF.R. Concurrently, increased RD values were observed in the IFO.L and SLF.R, along with increased MD values in the FMi, IFO.L, IFO.R, and SLF.R. These findings suggest that compensatory changes in white matter microstructure begin to occur in PA patients with normal cognitive function, providing a basis for further research into the mechanisms underlying PA-related brain changes and their clinical implications.

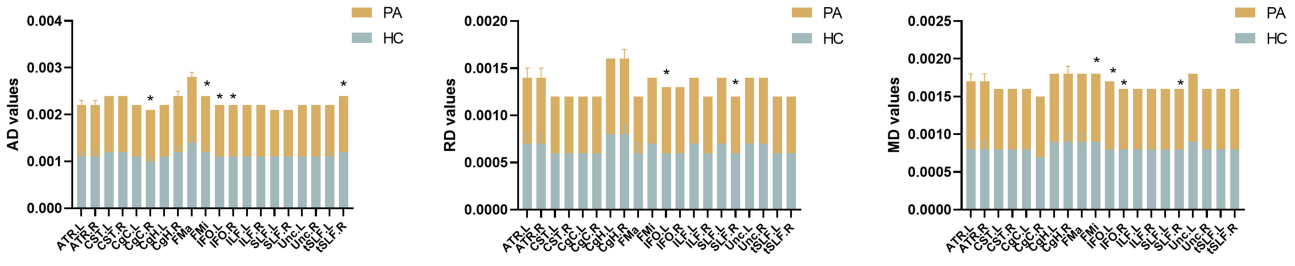

Figure 1 Comparison of DTI parameters with positive results between the PA and HC groups. The PA group demonstrated a notable increase in AD in the CgC.R, FMi, IFO.L, IFO.R and tSLF.R regions compared to the HC group. * denotes statistically significant differences between the groups.

Abbreviations: AD, axial diffusivity; RD, radial diffusivity; MD, mean diffusivity; HC, healthy controls; PA, primary aldosteronism; L, left; R, right; ATR, anterior thalamic radiation; CST, corticospinal tract; CgC, cingulum bundle cingulate part; CgH, cingulum bundle hippocampal part; FMa, forceps major; FMi, forceps minor; IFO, inferior fronto-occipital fasciculus; ILF, inferior longitudinal fasciculus; SLF, superior longitudinal fasciculus; Unc, uncinate fasciculus; tSLF, temporo-superior longitudinal fasciculus.

https://doi.org/10.2147/IJGM.S499346

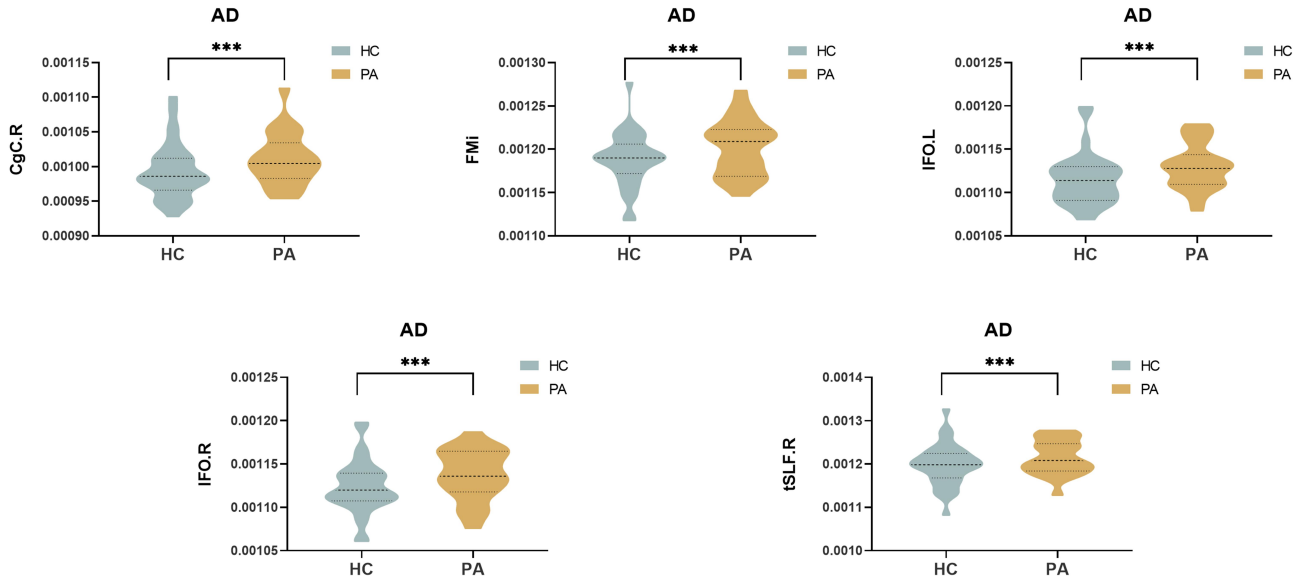

Figure 2 Comparison of AD values revealed significant differences between the HC and PA groups. The PA group demonstrated a notable increase in AD in the CgC.R, FMi, IFO.L, IFO.R and tSLF.R regions compared to the HC group. *** denotes statistically significant differences between the groups.
Abbreviations: AD, axial diffusivity; HC, healthy controls; PA, primary aldosteronism; L, left; R, right; CgC, cingulum bundle cingulate part; FMi, forceps minor; IFO, inferior fronto-occipital fasciculus; tSLF, temporo-superior longitudinal fasciculus.

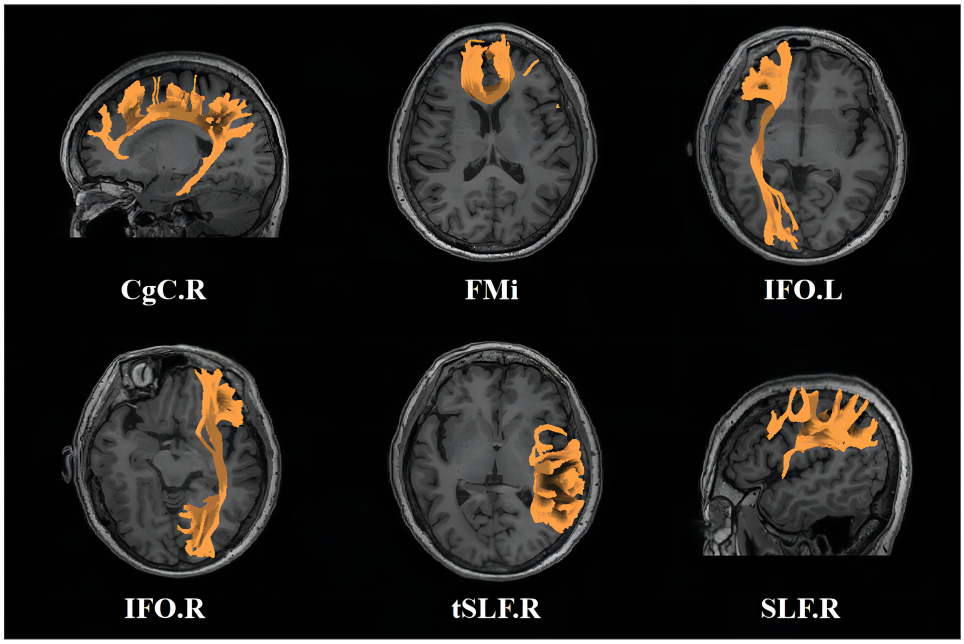

Figure 3 There are differences in the white matter microstructural alterations between the HC and PA group.
Abbreviations: HC, healthy controls; PA, primary aldosteronism; CgC.R, right cingulum bundle cingulate part; FMi, forceps minor; IFO.L, left inferior fronto-occipital fasciculus; IFO.R, right inferior fronto-occipital fasciculus; tSLF.R, right temporo-superior longitudinal fasciculus; SLF.R, right superior longitudinal fasciculus.

An increase in AD values indicates an enhanced ability of water molecules to diffuse along the main axis of nerve fibers, possibly reflecting a more intact or compact axial microstructure of nerve fibers.[9] The observed increase in MD values across several regions, as an average measure of diffusivity in all directions, implies a possible increase in tissue density or improved myelin integrity.[10] Meanwhile, an increase in RD values, which measures diffusion perpendicular to the main axis of nerve fibers, typically signifies less restricted perpendicular diffusion, suggesting possible demyelination or less compact myelin structure. These changes may reflect alterations in the structure of nerve fiber axons and potential

Table 4 Comparison of RD Values Between the Two Groups Based on ROIs ($\bar{x}$ ± s)

ROIs	PA	HC	*p* value	t value
ATR.L	0.0007 ± 0.0001	0.0007 ± 0.0001	0.8488	0.1916
ATR.R	0.0007 ± 0.0001	0.0007 ± 0.0001	0.4206	0.8117
CST.L	0.0006 ± 0.0000	0.0006 ± 0.0000	0.2959	1.0558
CST.R	0.0006 ± 0.0000	0.0006 ± 0.0000	0.4015	0.8457
CgC.L	0.0006 ± 0.0000	0.0006 ± 0.0000	0.5375	−0.6207
CgC.R	0.0006 ± 0.0000	0.0006 ± 0.0000	0.5491	0.6030
CgH.L	0.0008 ± 0.0000	0.0008 ± 0.0000	0.1124	1.6142
CgH.R	0.0008 ± 0.0001	0.0008 ± 0.0001	0.3561	0.9309
FMa	0.0006 ± 0.0000	0.0006 ± 0.0001	0.3165	1.0113
FMi	0.0007 ± 0.0000	0.0007 ± 0.0000	0.0558	1.9558
IFO.L	0.0007 ± 0.0000	0.0006 ± 0.0000	**0.0169***	2.4670
IFO.R	0.0007 ± 0.0000	0.0006 ± 0.0000	0.0657	1.8792
ILF.L	0.0007 ± 0.0000	0.0007 ± 0.0000	0.0660	1.8771
ILF.R	0.0006 ± 0.0000	0.0006 ± 0.0000	0.0964	1.6924
SLF.L	0.0007 ± 0.0000	0.0007 ± 0.0000	0.1443	1.4820
SLF.R	0.00064 ± 0.0000	0.00062 ± 0.0000	**0.0153***	2.5071
Unc.L	0.0007 ± 0.0000	0.0007 ± 0.0000	0.8652	0.1706
Unc.R	0.0007 ± 0.0000	0.0007 ± 0.0000	0.1560	1.4390
tSLF.L	0.0006 ± 0.0000	0.0006 ± 0.0000	0.6611	−0.4409
tSLF.R	0.0006 ± 0.0000	0.0006 ± 0.0000	0.8280	−0.2183

Note: The data is presented as mean ± standard deviation. Bold and * indicates a significant difference between groups (p value < 0.05).

Abbreviations: RD, radial diffusivity; ROIs, regions of interest; PA, primary aldosteronism; HC, healthy controls; L, left; R, right; ATR, anterior thalamic radiation; CST, corticospinal tract; CgC, cingulum bundle cingulate part; CgH, cingulum bundle hippocampal part; FMa, forceps major; FMi, forceps minor; IFO, inferior fronto-occipital fasciculus; ILF, inferior longitudinal fasciculus; SLF, superior longitudinal fasciculus; Unc, uncinate fasciculus; tSLF, temporo-superior longitudinal fasciculus.

myelin repair in specific brain regions of PA patients. The elevated aldosterone levels in PA may compromise the blood-brain barrier (BBB) integrity, triggering oxidative stress and inflammation, which could further alter the brain's microenvironment and promote white matter repair.[15] Additionally, aldosterone may influence myelin formation or repair processes, facilitating axonal and myelin regeneration.[15] These mechanisms may collectively contribute to the observed white matter changes in PA patients.

The CgC.R, located at the core of the brain and forming part of the limbic system, spans both hemispheres and is connected to other brain regions via the cingulum bundle. This bundle facilitates communication between internal brain regions.[21] The cingulate cortex plays a crucial role in various brain functions, including emotional regulation, pain processing, memory construction and retrieval, and self-referential thinking.[22] In the right hemisphere, the cingulate cortex is particularly associated with the regulation of negative emotions, pain perception, and social behavior management. It also involves cognitive functions such as attention focus and decision making.[23] Previous studies have shown

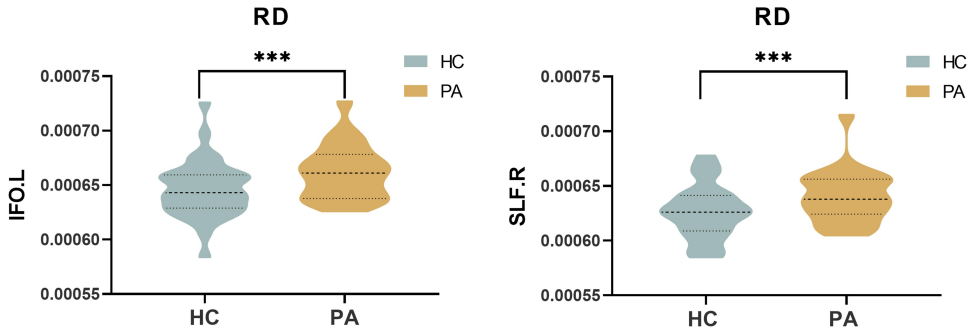

Figure 4 Comparison of RD values revealed significant differences between the HC and PA groups. The PA group demonstrated a notable increase in RD in the IFO.L and SLF.R regions compared to the HC group. *** denotes statistically significant differences between the groups.
Abbreviations: RD, radial diffusivity; HC, healthy controls; PA, primary aldosteronism; L, left; R, right; IFO, inferior fronto-occipital fasciculus; SLF, superior longitudinal fasciculus.

changes in the cingulate cortex in patients with cognitive decline and Alzheimer's disease.[24,25] Our study's observed increase in AD values in the CgC.R of PA patients suggests potential compensatory changes related to cognitive function.

FMi originates from the corpus callosum and extends forward to the frontal lobe, facilitating connections between various regions of the corpus callosum and the frontal lobe, thereby promoting information exchange between the brain's

Table 5 Comparison of MD Values Between the Two Groups Based on ROIs ($\bar{x}$ ± s)

ROIs	PA	HC	*p* value	t value
ATR.L	0.0009 ± 0.0001	0.0008 ± 0.0001	0.7946	0.2617
ATR.R	0.0009 ± 0.0001	0.0008 ± 0.0001	0.3604	0.9226
CST.L	0.0008 ± 0.0000	0.0008 ± 0.0000	0.4330	0.7901
CST.R	0.0008 ± 0.0000	0.0008 ± 0.0000	0.2515	1.1594
CgC.L	0.0008 ± 0.0000	0.0008 ± 0.0000	0.7658	−0.2994
CgC.R	0.0008 ± 0.0000	0.0007 ± 0.0000	0.1463	1.4744
CgH.L	0.0009 ± 0.0000	0.0009 ± 0.0000	0.1682	1.3971
CgH.R	0.0009 ± 0.0001	0.0009 ± 0.0001	0.3030	1.0402
FMa	0.0009 ± 0.0001	0.0009 ± 0.0001	0.3591	0.9251
FMi	0.0009 ± 0.0000	0.0008 ± 0.0000	**0.0463***	2.0403
IFO.L	0.00082 ± 0.0000	0.00080 ± 0.0000	**0.0070***	2.8040
IFO.R	0.00081 ± 0.0000	0.00080 ± 0.0000	**0.0243***	2.3191
ILF.L	0.0008 ± 0.0000	0.0008 ± 0.0000	0.1646	1.4092
ILF.R	0.0008 ± 0.0000	0.0008 ± 0.0000	0.0531	1.9783
SLF.L	0.0008 ± 0.0000	0.0008 ± 0.0000	0.1224	1.5698
SLF.R	0.00077 ± 0.0000	0.00075 ± 0.0000	**0.0152***	2.5090
Unc.L	0.0009 ± 0.0000	0.0009 ± 0.0000	0.4552	0.7523
Unc.R	0.0008 ± 0.0000	0.0008 ± 0.0000	0.1101	1.6250

(*Continued*)

Table 5 (Continued).

ROIs	PA	HC	*p* value	t value
tSLF.L	0.0008 ± 0.0000	0.0008 ± 0.0000	0.8362	0.2078
tSLF.R	0.0008 ± 0.0000	0.0008 ± 0.0000	0.4698	0.7280

Note: The data is presented as mean ± standard deviation. Bold and * indicates a significant difference between groups (p value < 0.05).

Abbreviations: MD, mean diffusivity; ROIs, regions of interest; PA, primary aldosteronism; HC, healthy controls; L, left; R, right; ATR, anterior thalamic radiation; CST, corticospinal tract; CgC, cingulum bundle cingulate part; CgH, cingulum bundle hippocampal part; FMa, forceps major; FMi, forceps minor; IFO, inferior fronto-occipital fasciculus; ILF, inferior longitudinal fasciculus; SLF, superior longitudinal fasciculus; Unc, uncinate fasciculus; tSLF, temporo-superior longitudinal fasciculus.

hemispheres. The corpus callosum is a critical fiber pathway connecting the two hemispheres, primarily transmitting information to the frontal lobe and other cortical areas through its radiations, particularly the anterior radiations.[26] FMi is crucial in processing high-level cognitive tasks, including decision-making, emotional regulation, attention management, and executive functions, especially in complex cognitive activities and emotional regulation.[27] Research has indicated changes in the fiber structure of FMi in Alzheimer's disease patients, highlighting its central role in cognitive processes.[28]

The IFO, spanning the lateral side of the brain, originates from the lower part of the frontal lobe, traverses the white matter region adjacent to the lateral ventricle, and extends to the lower part of the occipital lobe.[29,30] The IFO is essential in visual information processing and integrating complex cognitive functions, particularly in advanced visual recognition tasks.[31] It is closely related to language processing, comprehension, and executive functions, particularly in handling multimodal information integration and complex cognitive challenges.[32] Research on the IFO has enhanced our understanding of how the brain integrates visual information with higher-order cognitive functions.[33] Structural or functional changes in the IFO are closely associated with various neuropsychiatric disorders, such as Alzheimer's disease, autism spectrum disorders, and schizophrenia.[34–36] Studies have shown that alterations to the IFO in Alzheimer's patients is related to declines in visual

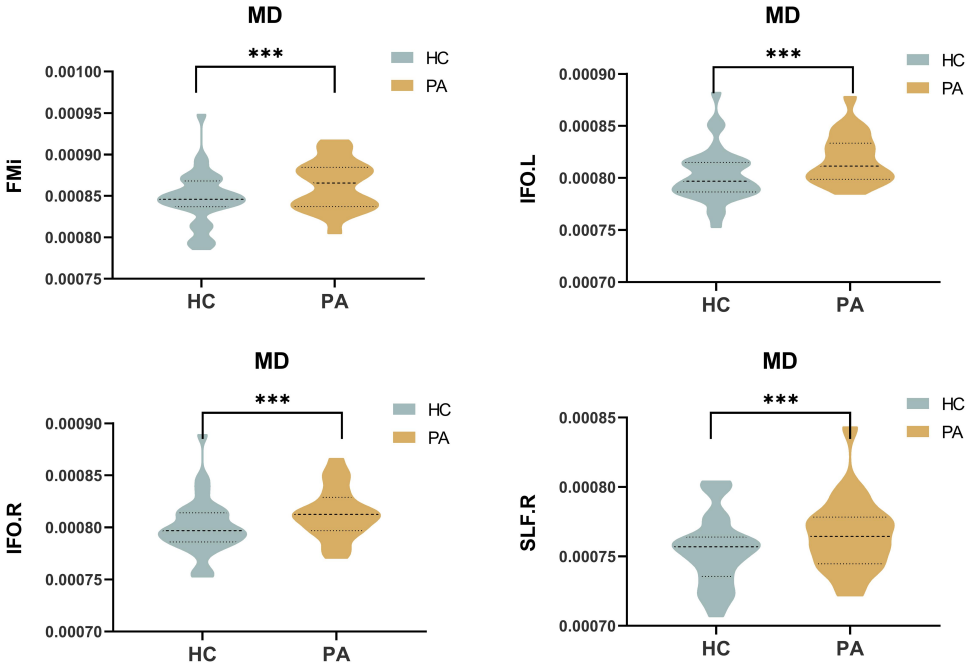

Figure 5 Comparison of MD values revealed significant differences between the HC and PA groups. The PA group demonstrated a notable increase in MD in the FMi, IFO.L, IFO.R, and SLF.R regions compared to the HC group. *** denotes statistically significant differences between the groups.

Abbreviations: MD, mean diffusivity; HC, healthy controls; PA, primary aldosteronism; L, left; R, right; FMi, forceps minor; IFO, inferior fronto-occipital fasciculus; SLF, superior longitudinal fasciculus.

https://doi.org/10.2147/IJGM.S499346

memory and spatial orientation abilities.[37] Furthermore, other studies have found that the IFO plays a role in language learning and processing, particularly impacting multilingual individuals and those with reading disorders.[31]

The tSLF.R, a long-distance white matter fiber bundle extending longitudinally on the right side of the brain, plays a key role in information transmission in the right hemisphere. It is primarily involved in language processing, visuospatial information, attention control, and processing social-emotional information.[38] In the right hemisphere, the tSLF.R is particularly responsible for processing non-verbal social-emotional information, such as facial expression recognition, spatial relationship processing, and the regulation of attention and visuospatial abilities.[39] Research on the function of tSLF.R is crucial for a deeper understanding of human social-emotional processing, spatial cognition, and language functions. The SLF.R traverses the lateral side of the brain, starting from the frontal lobe, passing through the parietal lobe, and reaching the temporal and occipital lobes. This fiber bundle comprises multiple subparts, each connecting different brain regions, thereby supporting various complex neural functions.[40] SLF.R is integral to several high-order cognitive functions, including language processing, attention control, visuospatial understanding, and working memory.[41] Especially in the right hemisphere, SLF.R is involved in processing non-verbal information such as spatial localization, facial expression recognition, and visuospatial skills, as well as emotional regulation and social cognitive processes.[42] Studies have shown that the structural integrity of SLF.R may be impaired in patients with autism spectrum disorders and schizophrenia, closely related to deficits in cognitive and social functions in these patients.[43–45]

This study's exploration of how PA affects white matter integrity is subject to several limitations, including a small sample size, cross-sectional study design, insufficient exploration of specific brain regions, and methodological differences across studies. These limitations hinder a comprehensive understanding of the mechanisms through which PA affects the brain. Although the sample size of 22 PA patients and 33 healthy controls is adequate for an exploratory study, larger cohorts are necessary for confirming these findings and improving generalizability. Furthermore, cross-sectional designs cannot establish causality, and longitudinal studies are needed to provide valuable insights into the progression of white matter changes over time. This would help in better understanding the dynamic relationship between PA and brain integrity. Moreover, the lack of research on specific brain regions limits our understanding of how PA impacts different functional areas of the brain. Methodological differences make it challenging to compare and synthesize results. Additionally, the lack of comparison with primary hypertensive patients limits our ability to determine whether the observed white matter changes are specific to PA or related to general hypertension. This study also did not include volumetric measurements of key brain structures, such as the corpus callosum, or examine correlations between white matter changes and renin-angiotensin-aldosterone system (RAAS) hormone levels, electrolyte imbalances, inflammatory markers, or the role of angiotensin II in myelin integrity due to data and sample limitations. Future research should address these areas to better understand PA's broader impact on the brain. Despite these challenges, studying changes in the white matter integrity of PA patients in specific brain regions, such as the CgC, the FMi, the bilateral IFO and the tSLF.R, remains of great value. These changes may be closely related to cognitive and emotional disorders in PA patients. Future research should aim to expand sample sizes, adopt longitudinal designs, conduct detailed analyses of specific brain regions, and standardize imaging and data processing methods to enhance the stability and broad applicability of the findings. This will provide more precise diagnostic, therapeutic, and prognostic assessments for PA patients.

Conclusion

Our study demonstrates that compensatory microstructural alterations in the white matter are evident in PA patients, even in the absence of cognitive impairment. These alterations are primarily indicated by increased AD, RD, and MD within specific brain region fiber tracts. These findings suggest that changes in white matter structure could serve as potential imaging biomarkers of brain alterations in PA patients with normal cognitive function. However, further studies are needed to determine whether these structural changes are indicative of future cognitive decline. We recommend integrating DTI into routine clinical evaluations for early detection and monitoring cognitive decline risk.

Data Sharing Statement

The data presented in this manuscript are part of the first author's doctoral dissertation. As much of the dissertation remains unpublished, sharing deidentified participant data at this stage could risk premature disclosure of unpublished

results and compromise ongoing research. Therefore, the authors regret that these data cannot be made available for sharing at this time.

Acknowledgments

This work was partially supported by the Dongguan Science and Technology of Social Development Program (Grant No. 20231800940052), the Dongguan Eighth People's Hospital Sponsorship Program (Grant No. DBBS2023005) and Key Laboratory of Coronary Intraluminal Imaging and Functional Analysis of Dongguan City, Dongguan, Guangdong, China.

Disclosure

The authors report no conflicts of interest in this work.

References

1. Ekman N, Grossman AB, Dworakowska D. What We Know About And What Is New In Primary Aldosteronism. *Int J Mol Sci*. 2024;25(2):900. doi:10.3390/ijms25020900
2. Charoensri S, Turcu AF. Primary aldosteronism prevalence - an unfolding story. *Exp Clin Endocrinol Diab*. 2023;131(7–08):394–401. doi:10.1055/a-2066-2696
3. Quencer KB, Rugge JB, Senashova O. Primary aldosteronism. *Am Family Phys*. 2023;108(3):273–277.
4. Mullen N, Curneen J, Donlon PT, et al. Treating primary aldosteronism-induced hypertension: novel approaches and future outlooks. *Endocrine Rev*. 2024;45(1):125–170. doi:10.1210/endrev/bnad026
5. Wartolowska KA, Webb AJS. Blood pressure determinants of cerebral white matter hyperintensities and microstructural injury: UK biobank cohort study. *Hypertension*. 2021;78(2):532–539. doi:10.1161/HYPERTENSIONAHA.121.17403
6. Filley CM, Fields RD. White matter and cognition: making the connection. *J Neurophysiol*. 2016;116(5):2093–2104. doi:10.1152/jn.00221.2016
7. Lope-Piedrafita S. Diffusion tensor imaging (DTI). *Methods Mol Biol*. 2018;1718:103–116.
8. Alexander AL, Lee JE, Lazar M, Field AS. Diffusion tensor imaging of the brain. *Neurotherapeutics*. 2007;4(3):316–329. doi:10.1016/j.nurt.2007.05.011
9. Figley CR, Uddin MN, Wong K, Kornelsen J, Puig J, Figley TD. Potential pitfalls of using fractional anisotropy, axial diffusivity, and radial diffusivity as biomarkers of cerebral white matter microstructure. *Front Neurosci*. 2021;15:799576. doi:10.3389/fnins.2021.799576
10. Debarle C, Perlbarg V, Jacquens A, et al. Global mean diffusivity: a radiomarker discriminating good outcome long term after traumatic brain injury. *Ann Phys Rehabil Med*. 2021;64(2):101433. doi:10.1016/j.rehab.2020.08.002
11. Jiménez-Balado J, Riba-Llena I, Abril O, et al. Cognitive impact of cerebral small vessel disease changes in patients with hypertension. *Hypertension*. 2019;73(2):342–349. doi:10.1161/HYPERTENSIONAHA.118.12090
12. Kim JS, Lee S, Suh SW, et al. Association of low blood pressure with white matter hyperintensities in elderly individuals with controlled hypertension. *J Stroke*. 2020;22(1):99–107. doi:10.5853/jos.2019.01844
13. Reas ET, Laughlin GA, Hagler DJ Jr, Lee RR, Dale AM, McEvoy LK. Age and sex differences in the associations of pulse pressure with white matter and subcortical microstructure. *Hypertension*. 2021;77(3):938–947. doi:10.1161/HYPERTENSIONAHA.120.16446
14. Wang L, Lin H, Zhao Z, et al. Sex disparity of cerebral white matter hyperintensity in the hypertensive elderly: the Shanghai Changfeng study. *Human Brain Mapp*. 2023;44(5):2099–2108. doi:10.1002/hbm.26196
15. Nieckarz A, Graff B, Burnier M, Marcinkowska AB, Narkiewicz K. Aldosterone in the brain and cognition: knowns and unknowns. *Front Endocrinol*. 2024;15:1456211. doi:10.3389/fendo.2024.1456211
16. Lin X, Ullah MHE, Wu X, et al. Cerebro-cardiovascular risk, target organ damage, and treatment outcomes in primary aldosteronism. *Front Cardiovasc Med*. 2021;8:798364. doi:10.3389/fcvm.2021.798364
17. Chen W, Deng S, Jiang H, Li H, Zhao Y, Yuan Y. Alterations of white matter connectivity in adults with essential hypertension. *Int J Gene Med*. 2024;17:335–346. doi:10.2147/IJGM.S444384
18. Reincke M, Bancos I, Mulatero P, Scholl UI, Stowasser M, Williams TA. Diagnosis and treatment of primary aldosteronism. *Lancet Diab Endocrinol*. 2021;9(12):876–892. doi:10.1016/S2213-8587(21)00210-2
19. Cui Z, Zhong S, Xu P, He Y, Gong G. PANDA: a pipeline toolbox for analyzing brain diffusion images. *Front Hum Neurosci*. 2013;7:42. doi:10.3389/fnhum.2013.00042
20. Hua K, Zhang J, Wakana S, et al. Tract probability maps in stereotaxic spaces: analyses of white matter anatomy and tract-specific quantification. *Neuroimage*. 2008;39(1):336–347. doi:10.1016/j.neuroimage.2007.07.053
21. Vogt BA. The cingulate cortex in neurologic diseases: history, structure, overview. *Handbook Clin Neurol*. 2019;166:3–21.
22. Bubb EJ, Metzler-Baddeley C, Aggleton JP. The cingulum bundle: anatomy, function, and dysfunction. *Neurosci Biobehav Rev*. 2018;92:104–127. doi:10.1016/j.neubiorev.2018.05.008
23. Mandl RC, van den Heuvel MP, Klomp DW, et al. Tract-based magnetic resonance spectroscopy of the cingulum bundles at 7 T. *Human Brain Mapp*. 2012;33(7):1503–1511. doi:10.1002/hbm.21302
24. Gozdas E, Fingerhut H, Chromik LC, O'Hara R, Reiss AL, Hosseini SMH. Focal white matter disruptions along the cingulum tract explain cognitive decline in amnestic mild cognitive impairment (aMCI). *Sci Rep*. 2020;10(1):10213. doi:10.1038/s41598-020-66796-y
25. Vlegels N, Ossenkoppele R, van der Flier WM, et al. Does loss of integrity of the cingulum bundle link amyloid-β accumulation and neurodegeneration in alzheimer's disease? *J Alzheimer's Dis*. 2022;89(1):39–49. doi:10.3233/JAD-220024
26. Ruiz-Rizzo AL, Viviano RP, Daugherty AM, Finke K, Müller HJ, Damoiseaux JS. Subjective cognitive decline predicts lower cingulo-opercular network functional connectivity in individuals with lower neurite density in the forceps minor. *Neuroimage*. 2022;263:119662. doi:10.1016/j.neuroimage.2022.119662

27. Porcu M, Cocco L, Cau R, et al. Correlation of cognitive reappraisal and the microstructural properties of the forceps minor: a deductive exploratory diffusion tensor imaging study. *Brain Topography*. 2024;37(1):63–74. doi:10.1007/s10548-023-01020-4
28. Zhang Y, Lin L, Feng M, et al. The mean diffusivity of forceps minor is useful to distinguish amnestic mild cognitive impairment from mild cognitive impairment caused by cerebral small vessel disease. *Front Hum Neurosci*. 2022;16:1010076. doi:10.3389/fnhum.2022.1010076
29. Wu Y, Sun D, Wang Y, Wang Y. Subcomponents and connectivity of the inferior fronto-occipital fasciculus revealed by diffusion spectrum imaging fiber tracking. *Front Neuroanatomy*. 2016;10:88. doi:10.3389/fnana.2016.00088
30. van Heesewijk J, Steenwijk MD, Kreukels BPC, Veltman DJ, Bakker J, Burke SM. Alterations in the inferior fronto-occipital fasciculus - a specific neural correlate of gender incongruence? *Psychol Med*. 2023;53(8):3461–3470. doi:10.1017/S0033291721005547
31. Rollans C, Cheema K, Georgiou GK, Cummine J. Pathways of the inferior frontal occipital fasciculus in overt speech and reading. *Neuroscience*. 2017;364:93–106. doi:10.1016/j.neuroscience.2017.09.011
32. Conner AK, Briggs RG, Sali G, et al. A connectomic atlas of the human cerebrum-chapter 13: tractographic description of the inferior fronto-occipital fasciculus. *Operative Neurosurg*. 2018;15(suppl_1):S436–s443. doi:10.1093/ons/opy267
33. Chen HF, Huang LL, Li HY, et al. Microstructural disruption of the right inferior fronto-occipital and inferior longitudinal fasciculus contributes to WMH-related cognitive impairment. *CNS Neurosci Ther*. 2020;26(5):576–588. doi:10.1111/cns.13283
34. Xiao D, Wang K, Theriault L, Charbel E. White matter integrity and key structures affected in Alzheimer's disease characterized by diffusion tensor imaging. *Eur J Neurosci*. 2022;56(8):5319–5331. doi:10.1111/ejn.15815
35. Kato Y, Kagitani-Shimono K, Matsuzaki J, et al. White matter tract-cognitive relationships in children with high-functioning autism spectrum disorder. *Psychiatry Invest*. 2019;16(3):220–233. doi:10.30773/pi.2019.01.16
36. Surbeck W, Hänggi J, Scholtes F, et al. Anatomical integrity within the inferior fronto-occipital fasciculus and semantic processing deficits in schizophrenia spectrum disorders. *Schizophr Res*. 2020;218:267–275. doi:10.1016/j.schres.2019.12.025
37. Mayo CD, Mazerolle EL, Ritchie L, Fisk JD, Gawryluk JR. Longitudinal changes in microstructural white matter metrics in Alzheimer's disease. *Neuroimage Clin*. 2017;13:330–338. doi:10.1016/j.nicl.2016.12.012
38. Petrušić I, Daković M, Kačar K, Mićić O, Zidverc-Trajković J. Migraine with aura and white matter tract changes. *Acta neurologica Belgica*. 2018;118(3):485–491. doi:10.1007/s13760-018-0984-y
39. Liu D, Liu Y, Hu X, et al. Alterations of white matter integrity associated with cognitive deficits in patients with glioma. *Brain Behav*. 2020;10(7):e01639. doi:10.1002/brb3.1639
40. Janelle F, Iorio-Morin C, D'Amour S, Fortin D. Superior longitudinal fasciculus: a review of the anatomical descriptions with functional correlates. *Front Neurol*. 2022;13:794618. doi:10.3389/fneur.2022.794618
41. Vergani F, Ghimire P, Rajashekhar D, F D, Lavrador JP. Superior longitudinal fasciculus (SLF) I and II: an anatomical and functional review. *J Neurosurg Sci*. 2021;65(6):560–565. doi:10.23736/S0390-5616.21.05327-3
42. de Oliveira JVM P, Raquelo-Menegassio AF, Maldonado IL. What's your name again? A review of the superior longitudinal and arcuate fasciculus evolving nomenclature. *Clin Anat*. 2021;34(7):1101–1110. doi:10.1002/ca.23764
43. Libero LE, Burge WK, Deshpande HD, Pestilli F, Kana RK. White matter diffusion of major fiber tracts implicated in autism spectrum disorder. *Brain Connect*. 2016;6(9):691–699. doi:10.1089/brain.2016.0442
44. Xu F, Jin C, Zuo T, Wang R, Yang Y, Wang K. Segmental abnormalities of superior longitudinal fasciculus microstructure in patients with schizophrenia, bipolar disorder, and attention-deficit/hyperactivity disorder: an automated fiber quantification tractography study. *Front Psychiatry*. 2022;13:999384. doi:10.3389/fpsyt.2022.999384
45. Koshiyama D, Fukunaga M, Okada N, et al. Association between the superior longitudinal fasciculus and perceptual organization and working memory: a diffusion tensor imaging study. *Neurosci lett*. 2020;738:135349. doi:10.1016/j.neulet.2020.135349